Journal of Electroceramics (2020) 44:215–222
https://doi.org/10.1007/s10832-020-00212-9

The electrical and optical properties of Nb-doping PLZT (9/65/35) transparent ceramics

Zhewei Xu[1,2] · Xia Zeng[1,3] · Zhaodong Cao[4] · Liang Ling[1,3] · Pingsun Qiu[1,3] · Xiyun He[1,3]

Received: 30 August 2019 / Accepted: 14 May 2020 / Published online: 22 May 2020

Abstract

In the past few decades, transparent electro-optical ceramics PLZT (9/65/35) ($Pb_{0.91}La_{0.09}(Zr_{0.65}Ti_{0.35})_{0.9775}O_3$) with special properties, particularly high transmittance in visible light, have gained much attention. However, restricted by the large ferroelectric hysteresis, the prospect is not optimistic. In this article, $Pb_{0.91}La_{0.09}(Zr_{0.65}Ti_{0.35})_{0.9775-5x/4}Nb_xO_3$ (abbreviated as PLZTN) transparent ceramics with varying Nb content ($x = 0.000, 0.005, 0.010, 0.015$) were fabricated by hot press sintering process under oxygen atmosphere. Electrical and optical properties were systematically studied. The temperature dependence of the dielectric constant showed a diffuse phase transition indicated typical relaxor behaviour. Moreover, the temperature at maximum dielectric constant (T_m) are near about 63 °C, almost unchanged. Comparing with undoped samples, the PLZTN with $x = 0.010$ Nb doping shows a dramatic reduction of 162.5% in ferroelectric hysteresis, with only a slight decrease in the maximum polarization from 30.04 μC/cm^2 to 28.53 μC/cm^2. The quadratic electro optic coefficient experienced 54.8% reduction but still satisfy the application requirements. In terms of transmittance, the PLZTN samples kept a high value of transmittance (about 64%) along with increasing Nb content. Hence, the conclusion can be drawn that Nb doping in PLZT (9/65/35) is a novel strategy to reduce the ferroelectric hysteresis.

Keywords Dielectric properties · Ferroelectric properties · Optical properties · Electro-optic properties · Hot pressing

1 Introduction

PLZT (lead lanthanum zirconate titanate) transparent ceramic has been studied for decades which was first synthesized and studied by CE Land and G Haertling in 1970 [1]. Benefited from the property of transparency, the electro-optic (EO) effect was discovered in the subsequent researches. The EO effect elaborates the relationship between the electric field applied and the refringence index of the ceramic (or single crystal) [2, 3]. PLZT (9/65/35) EO ceramic is a typical example with high quadratic EO coefficient. Depend on the large quadratic EO effect, it is widely used in applications such as light switch and optical modulator. However, a growing demand was proposed to optimizing the electrical and dielectrical properties. Therefore, it seems extremely important to put emphasis on modifications to the traditional PLZT ferroelectric ceramics, in which doping is the most commonly used method.

Much of the works have been published on doping. Ramam et al. [4] studied Sr, Mn doping in PLZT ceramics, and found the increase of dielectric constant and decrease of T_m. Xiucai Wang et al. [5] observed the lowering of dielectric loss in Ba doping PLZST. PLZT (9/65/35) with Bi/Cu co-doping was studied by S Somwan et al. [6], finding that the sintering temperature was brought down, and both coercive field and remnant polarization was decreased. Some other articles have discussed the effects of ca. [7], Fe [8], and rare earth elements [9]. In our previous work [10], the effects of La substitution on ferroelectric, dielectric and optic properties were fully studied, which is one of the rare works reported on PLZT quadratic EO effect.

The majority of the articles put the emphasis on piezoelectric, dielectric, pyroelectric properties and phase transition but seldom attach importance to the hysteresis. Although the PLZT (9/65/35) transparent EO ceramic shows an advantage of large quadratic EO coefficient, the hysteresis weakens its performance and becomes the greatest challenge for further

✉ Xiyun He
xyhe@mail.sic.ac.cn

1 Key Laboratory of Transparent Opto-Functional Inorganic Materials, Shanghai Institute of Ceramics, Chinese Academy of Sciences, 1295 Dingxi Road, 200050 Shanghai, China

2 University of Chinese Academy of Sciences, 100049 Beijing, China

3 Suzhou Research Institute, Shanghai Institute of Ceramics, Chinese Academy of Sciences, 6 Liangfu Road, 215400 Taicang, Jiangsu Province, China

4 Shanghai Institute of Laser Plasma, China Academy of Engineering Physics, 1129 Chengjiashan Road, 201800 Shanghai, China

applications. Generally, the hysteresis represents the size of the area enclosed by PE loop. Unless the area is zero, there are always two polarization values corresponding to one electric field value. This is troublesome to the designing of devices because an extra compensating circuit is needed. Hence, the unnoticed problem of hysteresis in PLZT (9/65/35) becomes prominent and is worth resolving. Just as mentioned above, no work has reported the issue of hysteresis in PLZT (9/65/35), not to mention the more crucial quadratic electro optic effect.

In this paper, Nb^{5+} ion was selected to modify the properties of PLZT (9/65/35) ceramics. Nb^{5+} addition that belongs to soft doping, creates vacancies which make the ions in the lattice more "active" and respond faster to the electric field. Additionally, the Nb doping give rise to the reduction of E_c as reported [11] and may further makes the *P-E* loop slimmer. PLZT (9/65/35) possesses a high value of transmittance and large quadratic electro optic coefficient which is the optimum candidate for electro optic devices. Thus, Nb doping PLZT ($Pb_{0.91}La_{0.09}(Zr_{0.65}Ti_{0.35})_{0.9775-5x/4}Nb_xO_3$) with $x = 0.000$, 0.005, 0.010, 0.015 (PLZTN) were fabricated by hot press atmosphere sintering process for the first time and the quadratic EO effect was studied as well. The study focused on solving the issue of large hysteresis and increasing the consistency which benefit greatly for the designing of devices and its further development.

2 Experiment

Metallic oxide powder of Nb_2O_5 (Shanghai, China; 99.99%), TiO_2 (Shanghai, China; 99.99%), ZrO_2 (Shanghai, China; 99.7%), La_2O_3 (Shanghai, China; 99.46%) and PbO (Sinopharm Chemical Reagent Co., Ltd Shanghai, China; 99.7%) were used in the experiment. Firstly, the precursor powder of ZrO_2-TiO_2 was obtained by weighting in molar ratio of 65/35 of the high pure TiO_2 and ZrO_2 raw powder, ball milling with alcohol before calcined at 800–900ºC. Then, PbO, La_2O_3 and Nb_2O_5 were added, ball milled again according to the formulation of $Pb_{0.91}La_{0.09}(Zr_{0.65}Ti_{0.35})_{0.9775-5x/4}Nb_xO_3$ with $x = 0.000$, 0.005, 0.010, 0.015, an excess 10 wt% of PbO was also added for the compensation of PbO loss during the sintering process. After that, 0.3 wt% of PVA as binder was added. Under the pressure of 18–20 MPa, the powder was pressed into cylinder before 12 h of sintering at 1200–1250 ºC by hot press atmosphere sintering process.

In order to match the needs of various measurements, the ceramics were tailored to certain sizes. The X-ray diffraction was employed to analyse the phase and lattice structure of the PLZTN samples in the range of 20–80º, (D/max 2550V, Japan). Scanning electron micrograph (Phenom-World BV Dillenburgstraat 9E; Netherlands) was used to observe the microstructure and estimate the grain sizes with 5000 magnification. E4990A Impedance Analyzer (Keysight, America) was used for the dielectric constant measurement from room temperature to about 300ºC, and Work Station equipment (Radiant Technologies, Albuquerque, New Mexico) for the estimate of ferroelectric properties under the frequency of 1 Hz. The experiment of transmittance was completed by the U2800 spectrophotometer (Hitachi, Tokyo, Japan) with sample thickness of about 0.3 mm. The study of quadratic electro-optic effect was carried out using He-Ne laser, details about the theory and testing process will be discussed later.

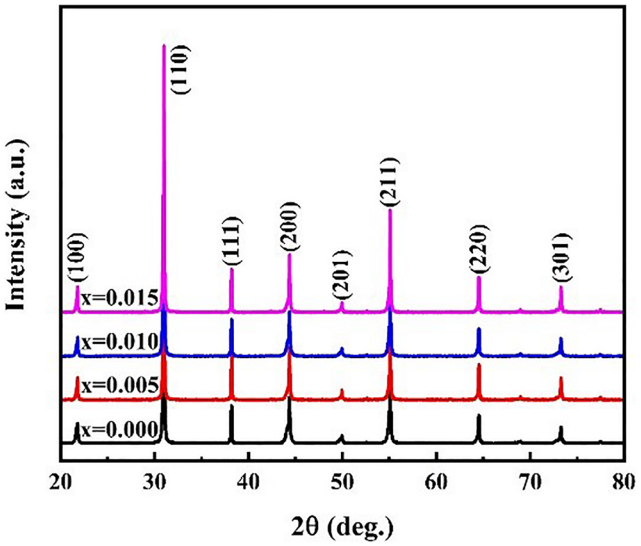

Fig. 1 X-ray diffraction patterns of PLZTN

3 Results and discussion

3.1 Phase structure

X-ray diffraction result was depicted in Fig. 1. No second phase can be observed within the detection limit and all the samples showed the pure perovskite phase structure. Due to the extremely small amount of Nb doping in the experiment, no obvious change in peak shift or intensity can be seen from the XRD pattern. Additionally, the pseudo cubic symmetry was determined based on the previous report [12] as well as

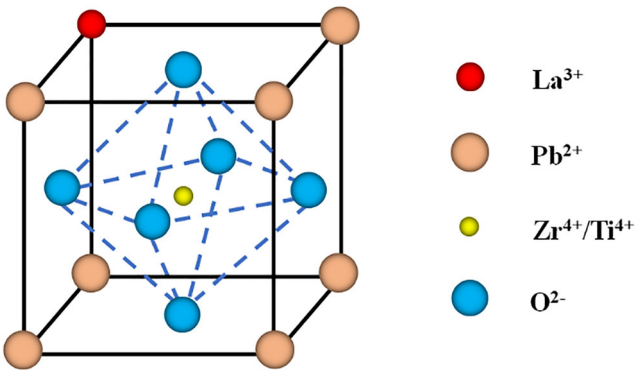

Fig. 2 Illustration of the ABO_3 perovskite structure

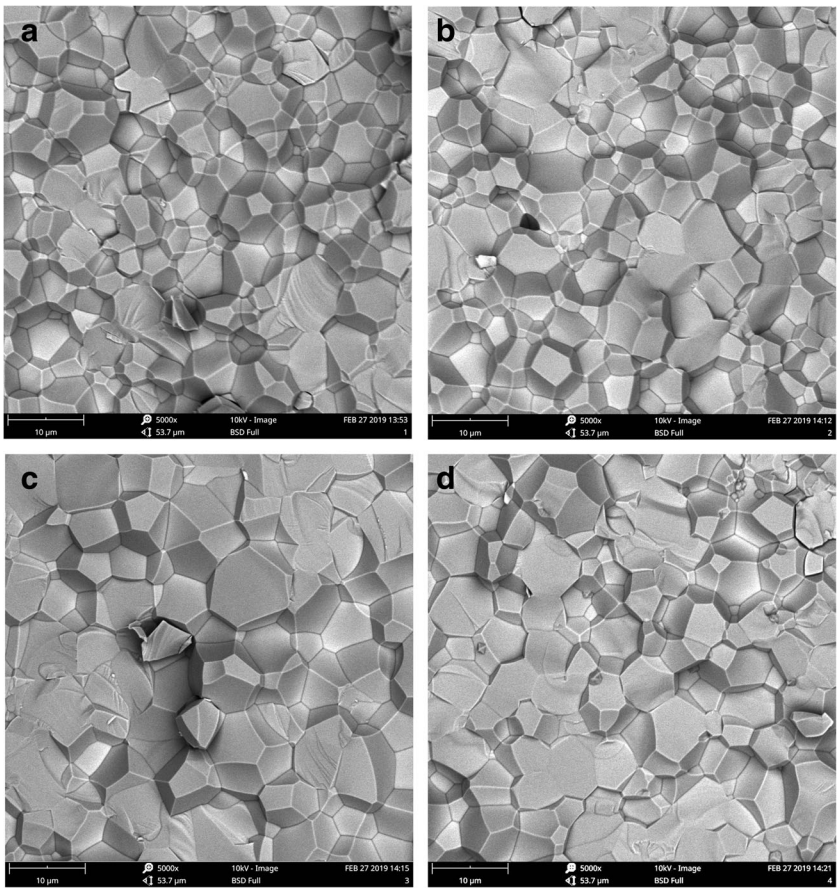

Fig. 3 SEM image of PLZTN with doping content of **a** 0.000, **b** 0.005, **c** 0.010 and **d** 0.015

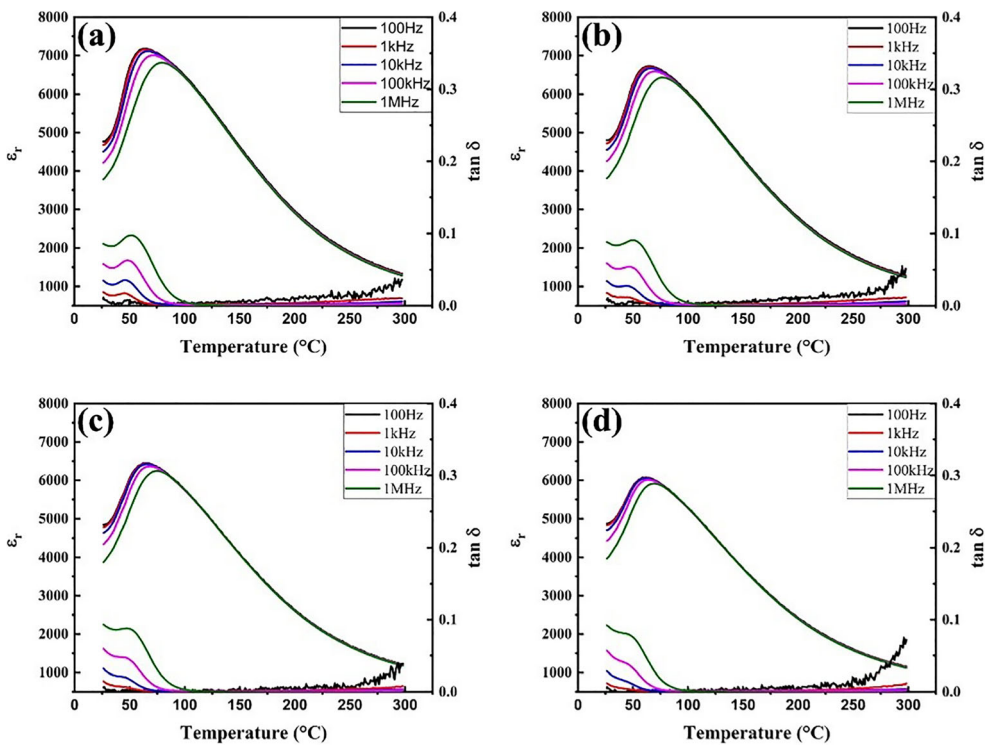

Fig. 4 Temperature dependence of dielectric constant and tan loss of PLZTN with doping content of (a) 0.000, (b) 0.005, (c) 0.010 and (d) 0.015 under the frequency of 100 Hz, 1 kHz, 10 kHz, 100 kHz and 1 MHz

the fact that the composition of PLZT (9/65/35) in the phase diagram located in the mixed phase region. In order to discuss the structure of PLZT (9/65/35), the ABO_3 perovskite structure should be introduced. Take PZT as the example of typical perovskite structure, Zr^{4+}/Ti^{4+} ions are set in the body central of the model occupying the 6 coordinated B site, whereas Pb^{2+} ions are set in the corner occupying the 12 coordinated A site, in addition, O^{2-} ions are set in the facial centre occupying the O site. Nevertheless, there is a little difference in PLZT, because the introduction of La^{3+} ions to the A site partially substitute Pb^{2+} ions (the larger ions preferred to occupy the A site in PZT [13]), as depicted in Fig. 2. Not only the difference in radius between La^{3+} and Pb^{2+} but also the electronic structure greatly influences the structure of ABO_3. Because of the higher valence of La^{3+} ions, the A site vacancies begin to appear which makes the structure more complex.

In order to evaluate the stability of the ABO_3 perovskite structure PLZTN lattice, the tolerance factor τ [14] was employed, which can be calculated by the following equation:

$$\tau = \frac{R_A + \mathrm{R_O}}{\sqrt{2}(R_B + \mathrm{R_O})} \tag{1}$$

In this formula, R_A, R_B and $\mathrm{R_O}$ represent for the average ion radius of the A site ions, the B site ions and O^{2-}, respectively. Furthermore, the average A site and B site ions' radii were calculated from the equations listed below:

$$R_A = 0.91\left(\mathrm{R_{Pb^{2+}}}\right) + 0.09\left(\mathrm{R_{La^{3+}}}\right) \tag{2}$$

$$R_B = (0.9775 - 5x/4) \times 0.65\mathrm{R_{Zr^{4+}}} + (0.9775 - 5x/4) \times 0.35\mathrm{R_{Ti^{4+}}} + x\mathrm{R_{Nb^{5+}}} \tag{3}$$

As reported in the previous works [15, 16], the radii of Pb^{2+}, La^{3+}, Zr^{4+}, Ti^{4+}, Nb^{5+} and O^{2-} mentioned above are 1.49 Å, 1.36 Å, 0.72 Å, 0.605 Å, 0.64 Å and 1.35 Å, respectively. From the information of ion radius, Nb^{5+} is closer to the B site Zr^{4+}/Ti^{4+} ions rather than the A site Pb^{2+}/La^{3+} ions, thus Nb^{5+} ion was supposed to enter the B site. Described by Park et al. [17], the τ of ABO_3 perovskite structure shall range from 0.9 to 1.1, and 1.0 is the value for idea perovskite structure. Besides, no perovskite structure may form beyond this range. What's more, the antiferroelectric phase is favoured when τ is no more than 1.0, otherwise, the ferroelectric structure is more stable. According to the equations above, the results calculated are 0.9927, 0.9933, 0.9939 and 0.9945, respectively, showed an increase, indicating the PLZTN ceramics prone to ferroelectric state [18].

3.2 Microstructure

The SEM image of PLZTN samples is depicted in Fig. 3a-d. From the SEM image, dense and uniform microstructure were observed. The average grain sizes estimated by linear intercept method from the SEM image are 4.41 μm, 4.56 μm, 4.74 μm and 5.40 μm, respectively. Obviously, the grain size shows an increasing tendency, which is due to that the Nb doping is still under the limit of solubility and enhances the solid-state chemical reaction [18, 19].

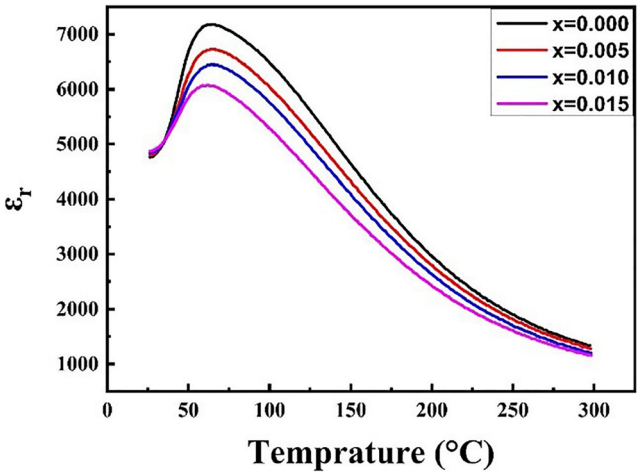

Fig. 5 Comparison of the ε-T curves of various doping content PLZTN under 100 Hz

3.3 Dielectric properties

Figure 4a-d shows the diagram of the relationship between dielectric constant ε, tanδ and temperature T, under the frequencies of 100 Hz, 1 kHz, 10 kHz, 100 kHz and 1 MHz. The typical diffuse phase transition (DPT) of peak broadening was observed, indicating PLZTN a relaxor ferroelectric. Figure 5 exhibits the ε-T diagram of PLZTN samples with varying doping amount under 100 Hz. The dielectric constant shows a decrease from about 7180 down to 6078 with increasing Nb content, and a linear decrease of the T_m was also observed. Further study of the diffuseness is necessary for relaxor, thus the degree of diffuseness γ was employed which can be calculated by the following equation [20]:

$$\frac{1}{\epsilon_r} - \frac{1}{\epsilon_m} = \frac{(T - T_m)^{\gamma}}{C} \tag{4}$$

ε_r, ε_m, T, T_m, γ and C proposed in Eq. (4) are the dielectric constant, the maximum dielectric constant,

Table 1 Results of ε_m and T_{m2}, and the degree of diffuseness (γ) and constant C calculated from linear fitting

Nb content	ε_m	T_m (°C)	γ	C ($\times 10^7$)
x = 0.000	7180	65.5	1.725	2.40
x = 0.005	6725	64.7	1.829	3.75
x = 0.010	6477	63.9	1.887	4.76
x = 0.015	6078	62.1	1.932	5.45

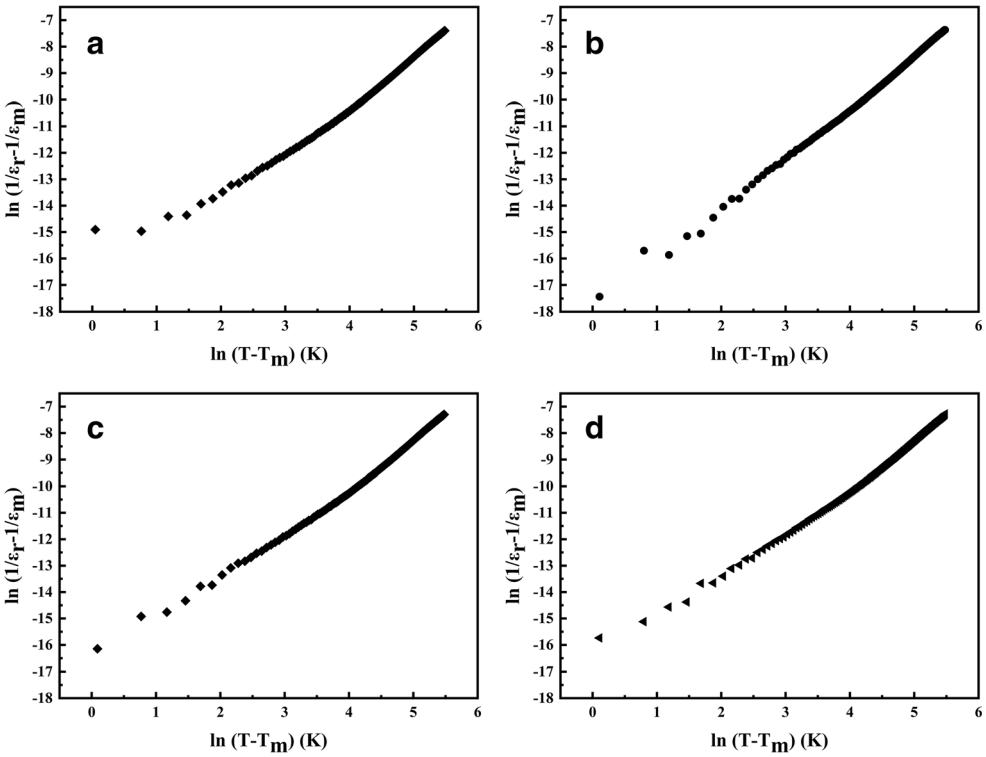

Fig. 6 $\ln(\frac{1}{\epsilon_r}-\frac{1}{\epsilon_m})$ versus $\ln(T-T_m)$ of PLZTN with doping content of **a** 0.000, **b** 0.005, **c** 0.010 and **d** 0.015 under 100 Hz

the temperature, the temperature at the maximum dielectric constant, the degree of diffuseness and a constant, respectively. The equation can be further changed into the formation as:

$$\ln\left(\frac{1}{\epsilon_r}-\frac{1}{\epsilon_m}\right)=\gamma\ln(T-T_m)-\ln C \quad (5)$$

From Eq. (5), the diagram of $\ln(\frac{1}{\epsilon_r}-\frac{1}{\epsilon_m})$ versus $\ln(T-T_m)$ is depicted in Fig. 6a-d, and then the γ and C were obtained according to the slope and the intercept through linear fitting. It is said that, for the nonrelaxor γ shall be 1, whereas 2 for completely relaxor. In this article, the values of dielectric constant versus

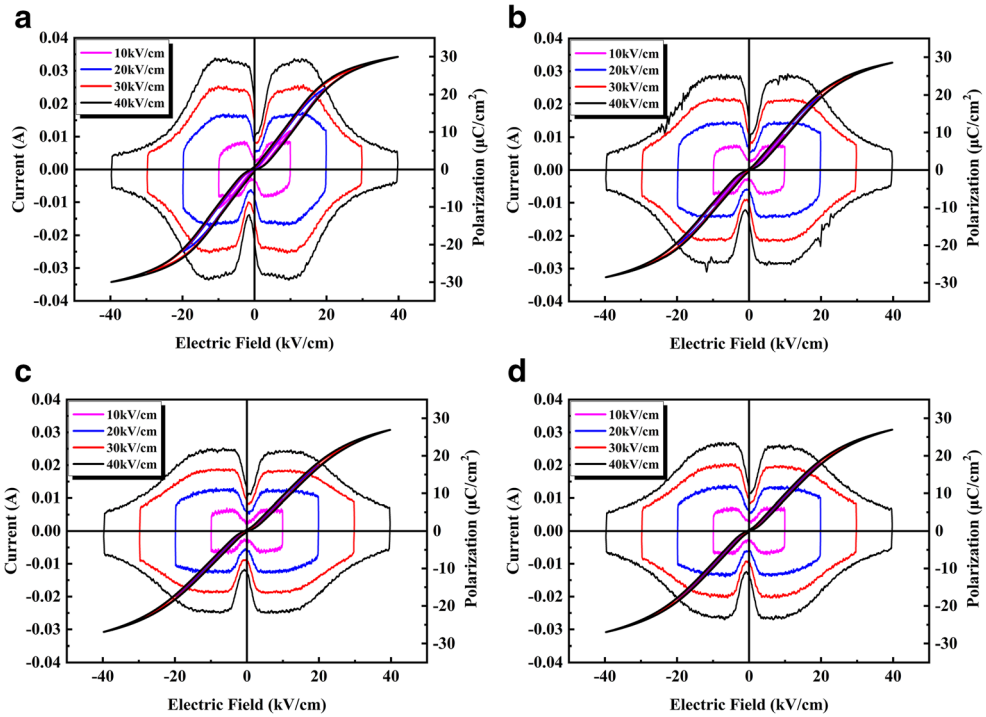

Fig. 7 The diagram of polarization and current versus electric field at room temperature of PLZTN with doping content of **a** 0.000, **b** 0.005, **c** 0.010 and **d** 0.015 under the measurement frequency of 1 Hz

temperature under 100 Hz were used in Eq. (5) and the results are shown in Table 1. Obviously, the γ has a positive correlation with Nb doping content, indicating an increasing tendency in disorder made by the mixing ions of Nb^{5+}, Zr^{4+} and Ti^{4+} that occupying the B site.

3.4 Ferroelectric properties

Figure 7a-d shows the plot of polarization and current versus electric field at room temperature and the details about E_c, P_r and P_{max} are listed in Table 2. The samples were tailored into the thickness of 0.5 mm and tested under the frequency of 1 Hz. Obviously, all these three parameters show a negative correlation tendency with doping content and the addition of Nb significantly reduce the P_r a lot as previously assumed. The dramatically decreased P_r indicated the enhancement of the domain mobility which was caused by two reasons. First is that the donor Nb^{5+} doping decreases the oxygen vacancies and polar defect complexes. Second is that the mixing ion effect of Zr^{4+}, Ti^{4+} and Nb^{5+} at the B site weakens the long-range order [21]. The enhancement of the domain mobility means that the ions are more active, less restricted and easier to make a displacement which is responsible for the increased repeatability of the *P-E* loop. Due to the shrink of the hysteresis loops at 0 kV/cm, the repeatability and the over-all properties can't be simply judged from the value of P_r and this will be discussed later together with the quadratic electro optic effect.

3.5 Optic, electro-optic properties

The transmittance of the PLZTN samples from 200 nm to 1100 nm is shown in Fig. 8. All the samples with the thickness of about 0.3 mm showed high transparency (about 61% at 632.8 nm) which is comparable to the 67% of PLDZT in the previous publication [22]. In this article, due to the small doping amount, PLZTN still keep the high transparency which is the prerequisite of the study on electro optic properties.

According to Haertling's theory [23] in evaluating the quadratic electro optic effect, the samples were set between the two crossed polarizer which were in 45°,

Table 2 Details about Ec, Pr and Pmax

Nb content	E_c (kV/cm)	P_r (μC/cm^2)	P_{max} (μC/cm^2)
x = 0.000	1.36	2.77	30.04
x = 0.005	0.56	0.74	29.96
x = 0.010	0.32	0.32	28.53
x = 0.015	0.39	0.36	26.92

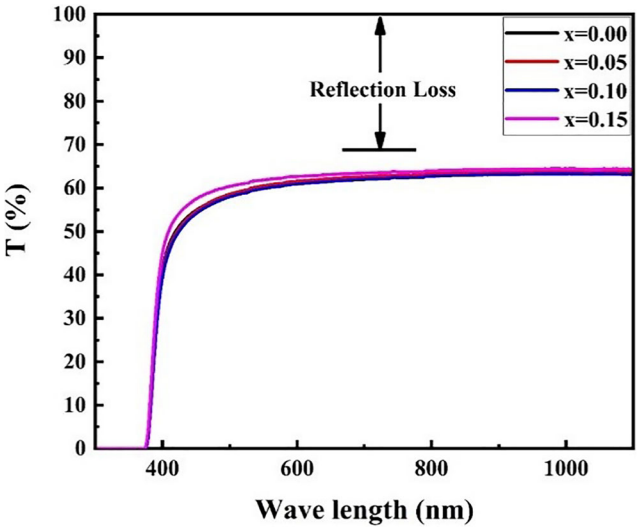

Fig. 8 Plot of transmittance of PLZTN, range from 200 nm to 1100 nm

the electric field was applied perpendicular to the optical path. Samples in this article were in the size of 2 × 6 × 3 mm^3 and He-Ne laser was employed as the 632.8 nm light source. The schematic diagram is depicted in Fig. 9 and the value of quadratic EO coefficient can be calculated by the following equations:

$$\frac{I}{I_0} = \sin^2\left(\frac{\pi l \Delta n}{\lambda}\right) \tag{6}$$

$$\Delta n = -\frac{1}{2} R n^3 E^2 \tag{7}$$

In the equations above, R is the quadratic EO coefficient. I_0, I, l, λ, n and E stand for the emergent light intensity, the incident light intensity, the length of the optical path, the wavelength, the refractive index (2.477 at 632.8 nm wavelength) and the electric field, respectively. The calculated R show a little decrease with increasing Nb doping and the details will be listed later.

In order to evaluate the relationship between hysteresis, quadratic EO coefficient and the Nb doping

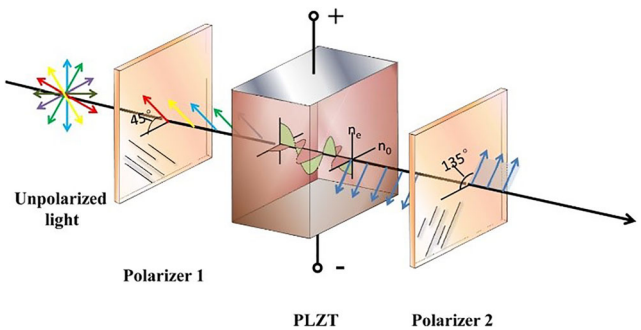

Fig. 9 Illustration of the quadratic electro optic effect based on Haertling's theory

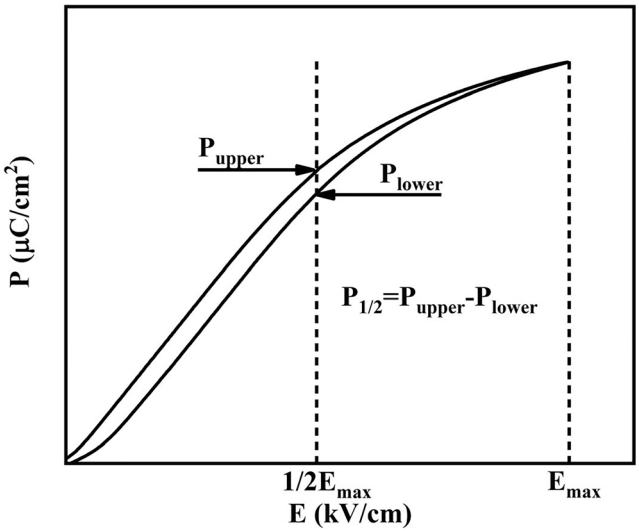

Fig. 10 Illustration of the $P_{1/2}$, P_{upper} and P_{lower}

amount more precisely, another calculation method was proposed. The difference between the two polarizations at the half maximum electric field (abbreviated as $P_{1/2}$) was used to judge the degree of hysteresis as illustrated in Fig. 10 and Eq. (8).

$$P_{1/2} = P_{upper} - P_{lower} \tag{8}$$

In Eq. (8), $P1_{/2}$, P_{upper} and P_{lower} represent for the difference value of P_{upper} and P_{lower} at half maximum the electric field, the upper value of polarization at the half maximum electric field and the lower value of polarization at the half maximum electric field, respectively. Based on the ferroelectric results of PLZTN with different doping amount, $P_{1/2}$ were calculated through Eq. (8), and the results are 4.2 μC/cm^2, 2.2 μC/cm^2, 1.6 μC/cm^2 and 1.4 μC/cm^2, respectively, details about $P_{1/2}$, P_{upper} and P_{lower} were listed in Table 3.

Obviously in Table 4, the PLZTN with x = 0.010 Nb doping amount exhibits the best improvement, which proves the assumption made before. Though the quadratic EO coefficient showed 54.8% decrease, still satisfy the application requirements and close to the 2.566×10^{-16} m^2/V^2 of PLDZT(10/65/35) [22], and the $P_{1/2}$ showed 162.5% decrease, comparing with x = 0.000. Accordingly, in this article, a novel method of Nb doping to resolve the problem of hysteresis in PLZT transparent ceramics was used and the result proves the correctness of the assumption.

Table 3 Details about P1/2, Pupper and Plower of PLZTN

Nb content	P_{upper}(μC/cm^2)	P_{lower}(μC/cm^2)	$P_{1/2}$(μC/cm^2)
x = 0.000	25.03	20.83	4.2
x = 0.005	23.52	21.32	2.2
x = 0.010	20.85	19.25	1.6
x = 0.015	18.30	16.90	1.4

Table 4 Quadratic electro optic coefficient of Nb5+ doping PLZT ceramics

Nb content	Quadratic electro optic coefficient ($\times 10^{-16}$ m^2/V^2)	$P_{1/2}$(μC/cm^2)
x = 0.000	1.44	4.2
x = 0.005	1.11	2.2
x = 0.010	0.93	1.6
x = 0.015	0.80	1.4

4 Conclusions

Transparent electro-optical ceramic PLZT (9/65/35) with x = 0.000, 0.005, 0.010, 0.015 Nb doping was synthesized by the hot press atmosphere sintering process, dense and fine-grained ceramics with high transmittance was obtained. XRD results clarified the PLZTN ceramics pure perovskite phase without second phase as well as the entrance of Nb^{5+} ions into the B site of the PLZT lattice. SEM image showed that the grain sizes had an increasing tendency, which was caused by the promotion of chemical reaction. Dielectric measurement exhibited an increase in the degree of diffuseness. As expected, Nb doping narrowed the hysteresis loop and increased the repeatability confirmed from the *P-E* loop, which was the main idea of this article. Considering the hysteresis, the transparency and the quadratic EO coefficient of x = 0.010 Nb doping, a conclusion can be made that the PLZTN ceramics is a promising material in electro-optic modulation devices.

Acknowledgements This work was financially supported by the National Natural Science Foundation of China (Grant No. 51602327) and the Institute Innovation Leading Special Project of Taicang (Jiangsu province, China) (Grant Nos. TC2018DYDS09).

References

1. C.E. Land, G.H. Haertiing 1970 J. Phys. Soc. Jap. **28** Suppl 96
2. A.R. Johnston, J.M. Weingart, JOSA **55**, 828–834 (1965)
3. X. Zeng et al., Ceram. Int. **40**, 6197–6202 (2014)
4. K. Ramam, K. Chandramouli, Ceram.-Silik. **53**, 189–194 (2009)
5. X.C. Wang et al., J. Mater. Sci.-Mater. Electron. **26**, 9200–9204 (2015)
6. S. Somwan, A. Ngamjarurojana, A. Limpichaipanit, Ceram. Int. **42**, 10690–10696 (2016)
7. S. Sen, R.N.P. Choudhary, P. Pramanik, Phys. B **387**, 56–62 (2007)
8. M.A. Mohiddon, K.L. Yadav, J. Phys. D-Appl. Phys. **40**, 7540 (2007)
9. S.R. Shannigrahi, F.E.H. Tay, K. Yao et al., J. Eur. Ceram. Soc. **24**, 163–170 (2004)
10. X. Zeng, W.X. Cheng, P.S. Qiu et al., Materials Science Forum. Trans Tech Publications **913**, 459–465 (2018)
11. S. Samanta, V. Sankaranarayanan, K. Sethupathi, J. Mater. Sci.-Mater. Electron. **29**, 20383–20394 (2018)

12. D.E. Dausch, Ferroelectric Polarization Fatigue in PZT-Based RAINBOWs and Bulk Ceramics[J]. J. Am. Ceram. Soc. **80**(9), 2355–2360 (1997)
13. M. Troccaz, P. Gonnard, L. Eyraud, Dopant distribution between A and B sites in PbZr0.95Ti0.05O3 ceramics of type ABO3[J]. Ferroelectrics **22**(1), 817–820 (1978)
14. S. Švarcová, K. Wiik, J. Tolchard et al., Solid State Ion. **178**, 1787–1791 (2008)
15. R.D. Shannon, Acta. Crystallogr. Sect. A **32**, 751–767 (1976)
16. R.D. Klissurska, K.G. Brooks, I.M. Reaney, C. Pawlaczyk, M. Kosec, N. Setter, J. Am. Ceram. Soc. **78**, 1513–1520 (1995)
17. S.E. Park, K. Markowski, S. Yoshikawa et al., J. Am. Ceram. Soc. **80** 407–412
18. M.A. Mohiddon, R. Kumar, P. Goel et al., IEEE Trns. Dielectr. Electr. Insul. **14**, 204–211 (2007)
19. B.W. Lee, E.J. Lee, J. Electroceram. **17**, 597–602 (2006)
20. X. Zeng, X. He, W. Cheng et al., J. Alloy. Compd. **485**, 843–847 (2009)
21. S. Samanta, V. Sankaranarayanan, K. Sethupathi, J. Mater. Sci.-Mater. Electron. **29**, 20383–20394 (2018)
22. X. Zeng, X. He, W. Cheng et al., Effect of Dy substitution on ferroelectric, optical and electro-optic properties of transparent Pb0. 90La0. 10 (Zr0. 65Ti0. 35) O3 ceramics[J]. Ceram. Int. **40**(4), 6197–6202 (2014)
23. G.H. Haertling, J. Am. Ceram. Soc. **82**, 797–818 (1999)